Real time single cell analysis of Bid cleavage and Bid translocation during caspase-dependent and neuronal caspase-independent apoptosis.

AUTHOR(S)

Manus W. Ward, Markus Rehm, Heiko Düssmann, Slavomir Kacmar, Caoimhin G. Concannon, Jochen HM Prehn

THE JOURNAL OF BIOLOGICAL CHEMISTRY VOL. 281, NO. 9, pp. 5837–5844, March 3, 2006

Real Time Single Cell Analysis of Bid Cleavage and Bid Translocation during Caspase-dependent and Neuronal Caspase-independent Apoptosis*

Received for publication, October 25, 2005, and in revised form, December 15, 2005 Published, JBC Papers in Press, December 28, 2005, DOI 10.1074/jbc.M511562200

Manus W. Ward, Markus Rehm, Heiko Duessmann, Slavomir Kacmar, Caoimhin G. Concannon, and Jochen H. M. Prehn[1]

From the Department of Physiology and Medical Physics and RCSI Neuroscience Research Centre, Royal College of Surgeons in Ireland, 123 St Stephen's Green, Dublin 2, Ireland

Bcl-2 homology domain (BH) 3-only proteins couple stress signals to evolutionarily conserved mitochondrial apoptotic pathways. Caspase 8-mediated cleavage of the BH3-only protein Bid into a truncated protein (tBid) and subsequent translocation of tBid to mitochondria has been implicated in death receptor signaling. We utilized a recombinant fluorescence resonance energy transfer (FRET) Bid probe to determine the kinetics of Bid cleavage and tBid translocation during death receptor-induced apoptosis in caspase 3-deficient MCF-7 cells. Cells treated with tumor necrosis factor-α (200 ng/ml) showed a rapid cleavage of the Bid-FRET probe occurring 75.4 ± 12.6 min after onset of the tumor necrosis factor-α exposure. Cleavage of the Bid-FRET probe coincided with a translocation of tBid to the mitochondria and a collapse of the mitochondrial membrane potential (ΔΨm). We next investigated the role of Bid cleavage in a model of caspase-independent, glutamate-induced excitotoxic apoptosis. Rat cerebellar granule neurons were transfected with the Bid-FRET probe and exposed to glutamate for 5 min. In contrast to death receptor-induced apoptosis, neurons showed a translocation of full-length Bid to the mitochondria. This translocation occurred 5.6 ± 1.7 h after the termination of the glutamate exposure and was also paralleled with a collapse of the ΔΨm. Proteolytic cleavage of the FRET probe also occurred, however, only 25.2 ± 3.5 min after its translocation to the mitochondria. Subfractionation experiments confirmed a translocation of full-length Bid from the cytosolic to the mitochondrial fraction during excitotoxic apoptosis. Our data demonstrate that both tBid and full-length Bid have the capacity to translocate to mitochondria during apoptosis.

The Bcl-2-homology domain-3 (BH3)[2]-only proteins are a subfamily of the Bcl-2 protein family involved in the initiation of apoptosis through the mitochondrial pathway (1, 2). The key event in the mitochondrial pathway is the release of proapoptotic factors from the mitochondrial intermembrane space into the cytosol (3) resulting in the downstream activation of a family of cytosolic cysteine proteases, caspases, that are required for many of the morphological changes that occur during apoptosis. The mitochondrial release of cytochrome-*c* and Smac/DIABLO allows for the formation of the apoptosome (4–6), a complex that enables the activation of caspases within the cell.

In many apoptotic models the proapoptotic Bcl-2 family members Bax or Bak are required for the release of caspase-activating factors from mitochondria (7). Both proteins are believed to form pores that make the outer mitochondrial membrane sufficiently permeable for the release of these intermembrane proteins (8). For this to occur, Bax and Bak must undergo conformational changes and insert into the outer mitochondrial membrane (9, 10). BH3-only proteins promote the activation of Bax and Bak either by direct protein association or through antagonizing the function of anti-apoptotic Bcl-2 family members (11).

The BH3-only protein Bid has been implicated in death receptor-induced apoptosis. In this pathway, Bid is post-translationally activated through caspase-8-mediated cleavage of the p22 FL-Bid protein to a truncated form (tBid) (12–14). This cleavage unmasks the BH3 domain, facilitating its accessibility for protein-protein interaction. tBid is subsequently myristoylated and translocates to mitochondria (15) to activate Bax or Bak (16, 17). The subsequent release of caspase-activating factors strongly amplifies caspase activation in response to death receptor ligation. Recently it has also become evident that Bid is critically involved in glutamate-induced apoptosis in neurons, as nerve cells from mice deficient in the BH3-only protein Bid are resistant to excitotoxic injury *in vitro* and ischemic injury *in vivo* (18, 19). Interestingly, excitotoxic apoptosis can proceed in the absence of detectable caspase activation (20–25) and hence represents a model of caspase-independent apoptosis in neurons. In the present study we have utilized single-cell real time imaging to examine the spatiotemporal profile of Bid expression and the kinetics of its activation during models of both caspase-dependent and caspase-independent apoptosis.

EXPERIMENTAL PROCEDURES

Materials—Fetal calf serum and minimal essential medium were purchased from Invitrogen. Recombinant human tumor necrosis factor-α (TNF-α), cycloheximide (CHX), glutamate, glycine, staurosporine, and all other reagents were from Sigma Fluo-4 AM and TMRM were purchased from Invitrogen.

Cell Culture—Human breast adenocarcinoma MCF-7 cells were cultured in RPMI 1640 medium (Invitrogen) supplemented with penicillin (100 units/ml), streptomycin (100 μg/ml), and 10% fetal calf serum (PAA, Cölbe, Germany). Cerebellar granule neurons were prepared as described previously (26) with minor modifications. Cerebella from 7-day-old Wistar rats of both sexes were dissected and pooled. The tissue was placed in 20 ml of filter-sterilized phosphate-buffered saline supplemented with 0.25 mg/ml trypsin and incubated at 37 °C for 20 min. Trypsinization was terminated by the addition of an equal volume of filter-sterilized phosphate-buffered saline supplemented with 0.05

* This work was supported by a grant from Science Foundation Ireland (03/RP/B344) (to J. H. M. P.). The costs of publication of this article were defrayed in part by the payment of page charges. This article must therefore be hereby marked "*advertisement*" in accordance with 18 U.S.C. Section 1734 solely to indicate this fact.

[1] To whom correspondence should be addressed: Dept. of Physiology and Medical Physics, Royal College of Surgeons in Ireland, 123 St Stephen's Green, Dublin 2, Ireland. Tel.: 353-1-402-2261; Fax: 353-1-402-2447; E-mail: Prehn@rcsi.ie.

[2] The abbreviations used are: BH3, Bcl-2-homology domain-3; FL-Bid, full-length Bid; TNF, tumor necrosis factor; CHX, cycloheximide; FRET, fluorescence resonance energy transfer; CFP, cyan fluorescent protein; YFP, yellow fluorescent protein; CHAPS, 3-[(3-cholamidopropyl)dimethylammonio]-1-propanesulfonic acid.

mg/ml soybean trypsin inhibitor, 3 mM $MgSO_4$, and 30 units/ml DNase I. The neurons were then triturated, and the resulting neurons were resuspended in supplemented culture medium. Cells were then plated on poly-L-lysine coated glass Willco dishes (Willco BV, Amsterdam, The Netherlands), 6-well plates and 24-well plates at 1×10^6 cells/ml and maintained at 37 °C in a humidified atmosphere of 5% CO_2:95% air.

Transfection—The pFRET-Bid plasmid was a kind gift from Dr. R. Onuki (National Institute of Advanced Industrial Science and Technology, Tsukuba, Japan) (27). MCF-7 cells were transfected with 0.6 μg of plasmid DNA (pFRET-Bid) and 6 μl of Lipofectamine 2000 (Invitrogen)/ml in serum-free culture medium at 37 °C for 3 h. For the generation of stable cell lines, transfected cells were selected in the presence of 1 mg/ml G418 (Stratagene, La Jolla, CA) for 2 weeks, and fluorescent clones were enriched. Cerebellar granule neurons were plated at 1×10^6 cells/ml on poly-L-lysine 2-cm glass-bottomed dishes. Half the medium was removed prior to transfection and retained for addition back to the neurons following the transfection. After 6–7 days, cerebellar granule neurons were transfected with pFRET-Bid plasmid using Lipofectamine 2000 according to the manufacturer's protocol. After 4–5 h in the transfection medium the cells were washed and returned to the preconditioned medium. Experiments were carried out 24–48 h after transfection.

Confocal Microscopy—MCF-7 cells stably transfected with the pFRET-Bid plasmid were cultivated in Hepes-buffered (10 mM, pH 7.4) RPMI 1640 medium. Apoptosis was induced with 200 ng/ml TNF-α/1 μg/ml CHX at the start of the measurements. Transfected cerebellar granule neurons were loaded with TMRM (30 nM) for 30 min at 37 °C (in the dark), in a buffered incubation medium (BM) consisting of 120 mM NaCl, 3.5 mM KCl, 0.4 mM KH_2PO_4, 20 mM HEPES, 5 mM $NaHCO_3$, 1.2 mM Na_2SO_4, 1.2 mM $MgCl_2$, 1.5 mM $CaCl_2$, and 15 mM glucose; pH 7.4. The Willco dishes with cells were washed in fresh medium after loading before being mounted in a non-perfusion (37 °C) holder and placed on the stage of a LSM 510 Meta Zeiss confocal microscope. No $MgCl_2$ was present in buffers for experiments that involved the addition of glutamate. Both types of cells were left to stabilize for 30 min prior to the start of an experiment. To observe FRET cleavage *in vitro*, neurons were transfected with a plasmid coding for the Bid-FRET probe and loaded with TMRM. CFP was excited at 405 nm with a 30 milliwatt laser diode adjusted to 2.5% of total intensity reflected by a 405/514 nm beam splitter. CFP and YFP (FRET-acceptor) emission were collected through 470–500 and 505–550 nm barrier filters, respectively. YFP was excited at 488 nm with an argon laser (1%), and the emission was collected through a 505–550 nm barrier filter. Cross-talk from CFP and YFP into the FRET channel was determined to be 33% of the CFP and 6% of the YFP fluorescence. There was no CFP cross-talk into the YFP channel. TMRM was excited with a helium neon laser (4%) at 543 nm, and the emission was collected with a 560 nm long pass filter. Images were taken at 5-min intervals and processed using Metamorph software. The TMRM emission signal was plotted as a percent of the total change following background subtraction. The standard deviation (S.D.) for the CFP and YFP emission signals were calculated. The changes in CFP S.D. were plotted as percent of the total change. Kinetics of FRET disruption were processed using Metamorph software (Universal Imaging, West Chester, PA), and the CFP/YFP emission ratios were obtained by dividing the integrated fluorescence intensity values of single cells (28). To compare individual cells, time courses of the emission ratios were scaled by defining the base-line ratio before the onset of FRET disruption as 0% and the ratio after termination of the FRET disruption as 100%. Plots were fitted with the sigmoidal Boltzmann equation $y = (A_1 - A_2)/(1 + \exp((x - x_0)/dt)) + A_2$ with dt determining the width of the turnover, A_1 the minimum, A_2 the maximum, and x_0 the time point when $(A_2 - A_1)/2$ is reached, using Origin 7.0 SRO (Origin Lab Corporation).

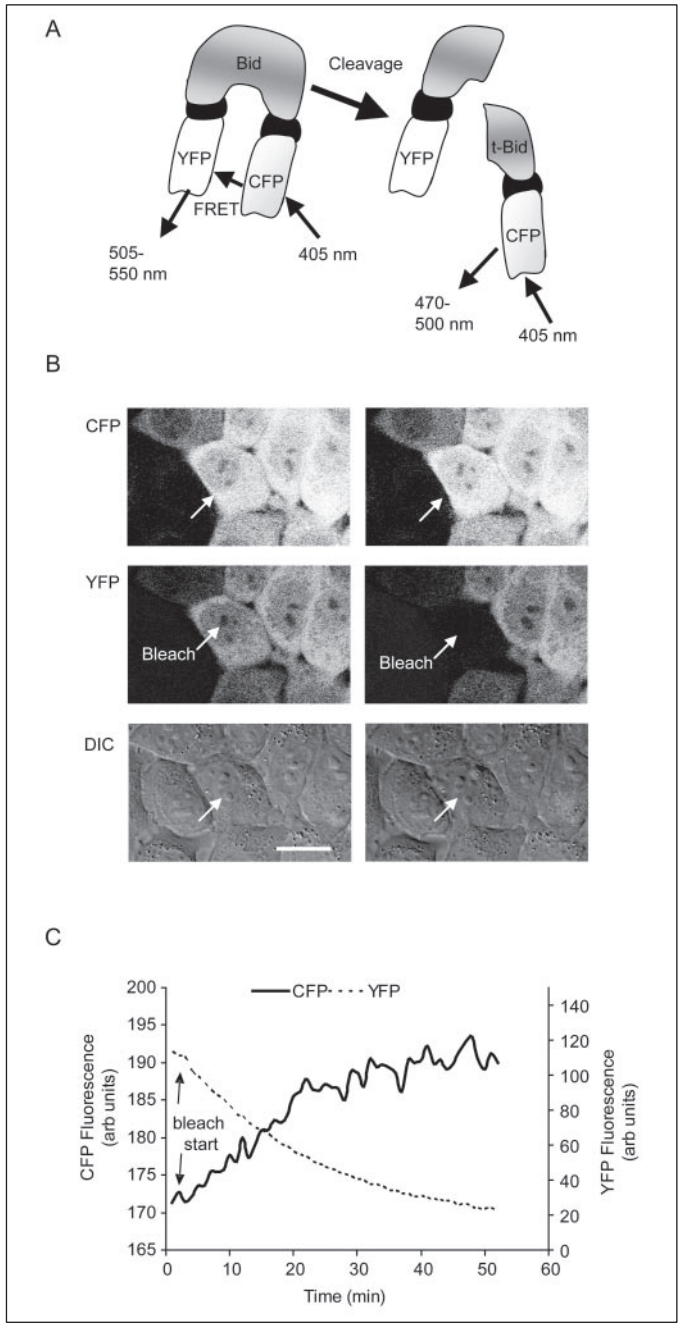

FIGURE 1. **Characterization of Bid FRET probe in MCF-7 cells.** *A*, Bid FRET system. CFP is excited at 405 nm, CFP emission is detected at 470–500 nm, and FRET emission is collected at 505–550 nm. Upon Bid cleavage, YFP is no longer in close proximity to CFP, resulting in a FRET decrease and a concomitant CFP fluorescence increase. *B–C*, acceptor bleaching confirms FRET between CFP and YFP. *B*, YFP was selectively bleached in a single cell by repeated scanning of the cell area at high laser power at 488 nm and 514 nm. Cellular morphology is shown in *DIC* images. *Bar* = 20 μm. The experiment was repeated twice. *C*, quantitative analysis of CFP and YFP fluorescence following the bleaching of YFP.

Detection of Cytosolic Ca^{2+} Transients—Cerebellar granule neurons on Willco dishes were co-loaded with TMRM (30 nM) and Fluo-4 AM (3 μM) for 30 min at 37 °C (in the dark), in BM. The Willco dishes with cells were washed in fresh medium after loading before being mounted in a non-perfusion (37 °C) holder and placed on the stage of a LSM 510 Meta Zeiss confocal microscope. No $MgCl_2$ was present in buffers for exper-

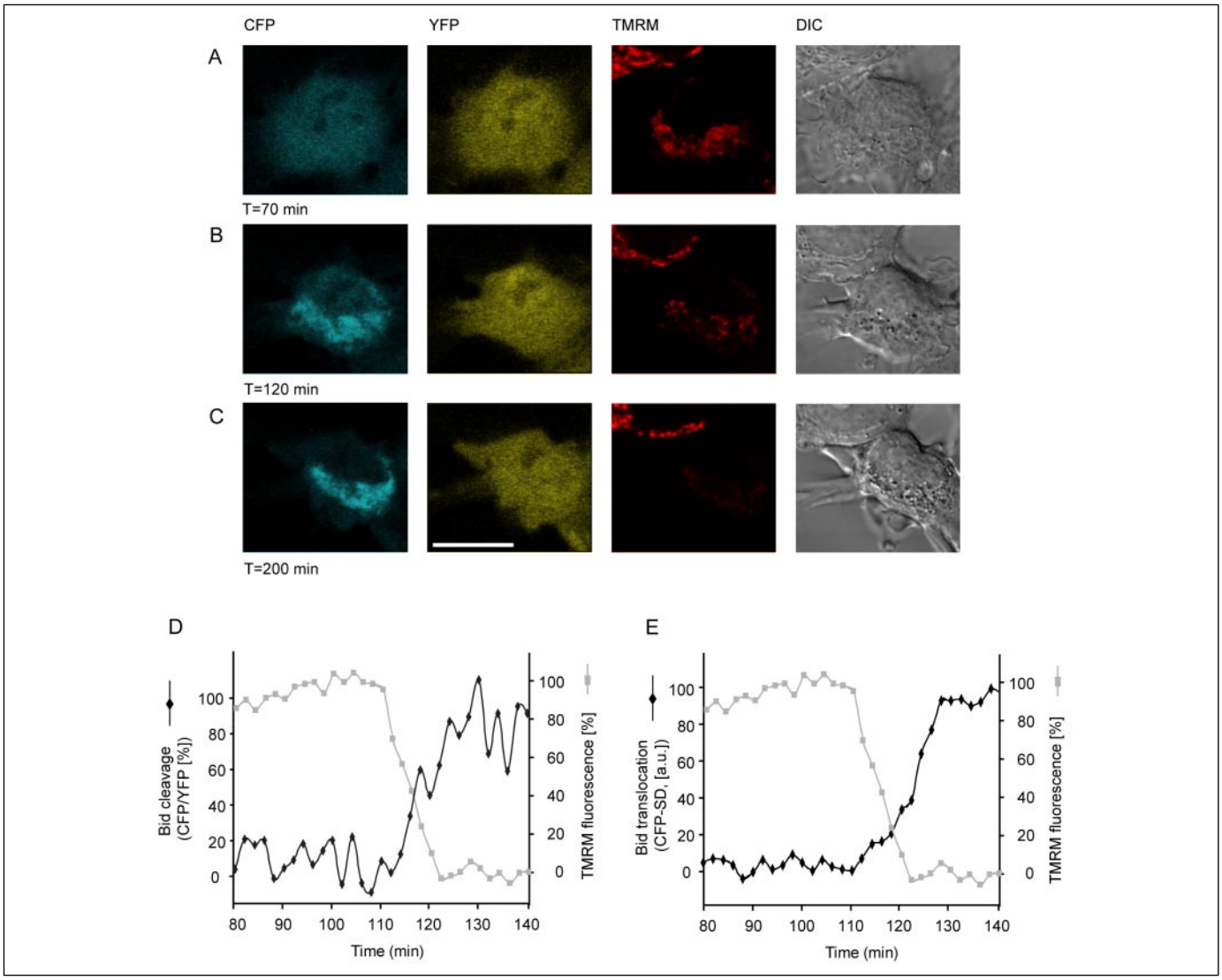

FIGURE 2. **Bid cleavage, translocation, and mitochondrial depolarization following death receptor activation in MCF-7 cells.** MCF-7 cells expressing the CFP-Bid-YFP FRET probe and loaded with 30 nM TMRM were treated with TNF-α/CHX (200 ng/ml, 1 μg/ml). The cells were monitored over time with images taken at 5 min intervals and the selected time points (70, 120, and 200 min) shown. *A*, time = 70 min, evenly distributed CFP and YFP fluorescence within the cell, polarized mitochondria (*TMRM*) normal cellular morphology (*DIC*). *B*, time = 120 min, clustering of CFP fluorescence, YFP fluorescence remains evenly distributed within the cell, partial depolarization of the ΔΨm (*TMRM*). *C*, time = 200 min, further clustering of CFP fluorescence, YFP fluorescence remains evenly distributed within the cell, depolarization of the ΔΨm (*TMRM*) and condensation of the cell (*DIC*). *D*, quantitative analysis of Bid cleavage (FRET disruption, CFP/YFP) and changes in the ΔΨm (TMRM fluorescence) following treatment with TNF-α/CHX (200 ng/ml/1 μg/ml). *E*, quantitative analysis of Bid translocation (CFP S.D.) and changes in the ΔΨm (TMRM fluorescence) following treatment with TNF-α. *n* = 37 cells from three separate experiments.

iments that involved the addition of glutamate. Fluo-4 AM was excited at 488 nm with an argon laser (1%), and the emission was collected through a 505–550 nm barrier filter, TMRM was excited at 543 nm with a helium neon laser (3%), and the emission was collected through a 560 nm long pass barrier filter. Images were collected every 60s and were processed using Metamorph software.

Lactate Dehydrogenase Release—Cerebellar granule neurons (1×10^6 cells/well) were plated on poly-L-lysine coated 24-well plates. In each case neuronal injury was assessed at each of the time points by quantitative measurement of lactate dehydrogenase release using a cytotoxicity detection kit (Roche Diagnostics). All conditions were carried out in triplicate in each experiment, and each experiment was carried out three times.

Digitonization, SDS-PAGE, and Western Blotting—Briefly, cells were permeabilized with 100 μg/ml digitonin at 4 °C for 10 min. The supernatant representing the cytosol and the mitochondria-containing pellet fraction were separated by centrifugation and denatured. SDS-PAGE and Western blot analysis was performed as described (Lankiewicz *et al.*, 22). Bid was detected with the rabbit polyclonal antibody (AR-53; 1:1,000), and Porin was detected by an anti-Porin mouse monoclonal antibody (Calbiochem) diluted 1:5000. Densitometric analysis was carried out on the Western blots using Metamorph software. The pixel intensity for each region was analyzed, the background was subtracted, and the FL-Bid expression was normalized to the porin loading control for each lane. The translocation of FL-Bid was then expressed as a percent of the control response.

Measurement of Caspase Activity—After treatment with glutamate/glycine (100 μM/10 μM), staurosporine (300 nM), or vehicle, the cerebellar granule neurons were lysed in 200 μl of lysis buffer. 50 μl of this lysate was added to 150 μl of reaction buffer (25 mM Hepes, 1 mM EDTA, 0.1% CHAPS, 10% sucrose, 3 mM dithiothreitol, pH 7.5) plus 10 μM caspase substrate, acetyl-Asp-Glu-Val-Asp-aminomethylcoumarin (Ac-DEVD-AMC), a fluorogenic substrate preferentially cleaved by caspase-3, -7, and -8 but also caspase-1, -6, -9, and -10 (28). Production

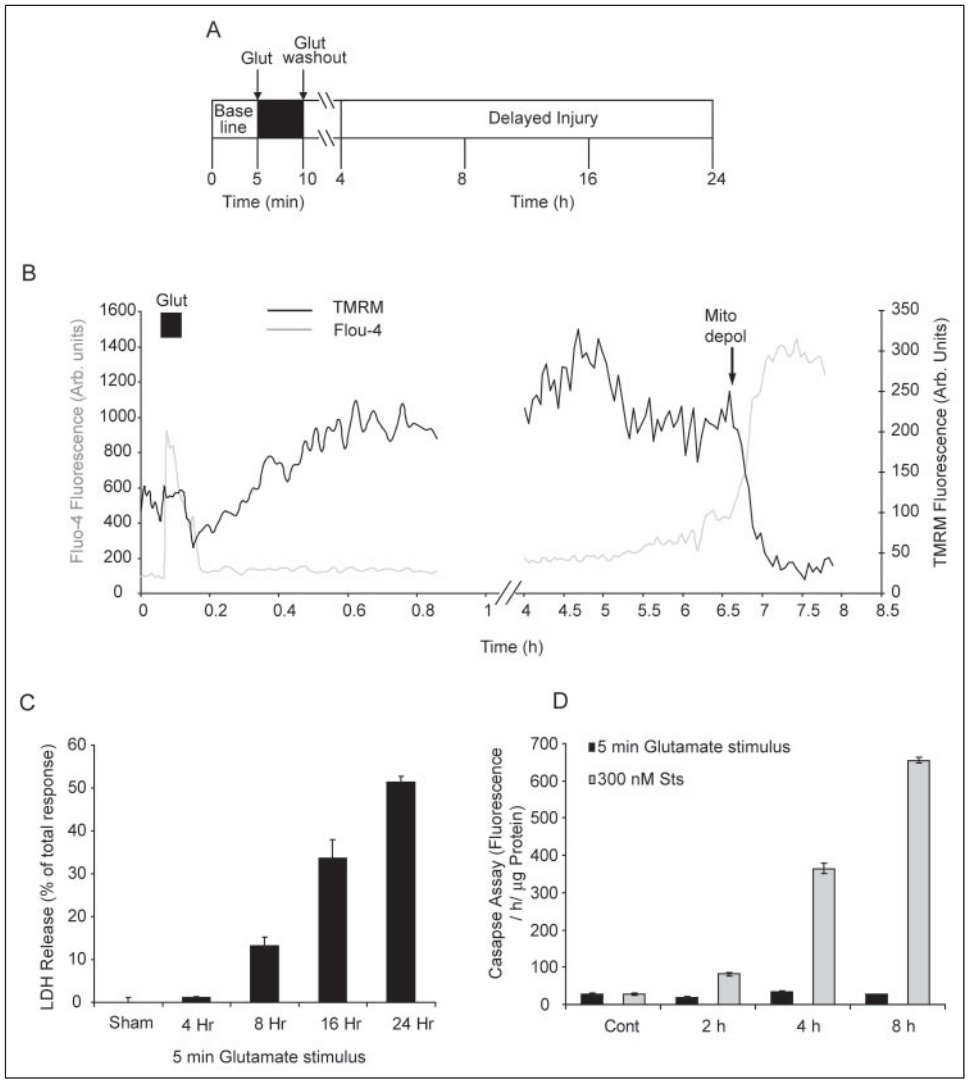

FIGURE 3. **Transient glutamate receptor overactivation induces a delayed caspase-independent neuronal injury.** *A*, flowchart for the experimental conditions used for the transient stimulation of cerebellar granule neurons with glutamate. Neurons are maintained in experimental buffer prior to glutamate stimulation (glutamate/glycine 100 μM/10 μM). Glutamate receptor activation is terminated after 5 min by washout of the glutamate stimulus or the addition of glutamate receptor antagonists (MK-801+NBQX 10 μM). *B*, cerebellar granule neurons were preloaded with TMRM (30 nM) and Fluo-4 AM (3 μM) for 30 min at 37 °C and stimulated with glutamate/glycine (100 μM/10 μM) for 5 min. MK-801 and NBQX (10 μM) were added to block glutamate receptor activation, and the neurons were monitored over time on a Zeiss LSM510 confocal microscope. *Arrows* indicate the onset of mitochondrial depolarization and loss of Ca^{2+} homeostasis. Traces are representative of responses in neurons from three separate experiments. *C*, cerebellar granule neurons were stimulated with glutamate/glycine as above (*A*), and LDH release was measured at indicated time points (4, 8, 16, and 24 h) following the initial insult ($n = 3$ experiments in triplicate). *D*, DEVD assay measuring caspase activation following transient glutamate receptor over activation (5 min glutamate/glycine 100 μM/10 μM) and treatment with staurosporine (*Sts*, 300 nM). There is no significant increase in caspase activation in neurons treated with glutamate ($n = 3$ experiments in triplicate).

of fluorescent aminomethylcoumarin was monitored over 60 min using a fluorescent plate reader (HTS 7000, PerkinElmer Life Science) (excitation 380 nm and emission 460 nm). Protein content was determined using the Pierce Coomassie Plus Protein Assay reagent (KMF, Cologne, Germany), and the caspase activity is expressed as change in fluorescent units/h/μg of protein.

Statistics—Data are given as means ± S.E. For statistical comparison, one-way analysis of variance followed by Tukey's test were employed. p values smaller than 0.05 were considered to be statistically significant.

RESULTS

Death Receptor Signaling in MCF-7 Cells Induces a Simultaneous Cleavage of Bid, Translocation of the Cleaved Bid, and Collapse in $\Delta\Psi m$—Caspase-mediated proteolytic activation of Bid has been demonstrated to be a key event in death receptor-mediated apoptosis (12, 13). However, analysis of this cleavage is complicated by the fact that both the initiator caspase-8 and the effector caspase-3 can cleave the protein (29). We took advantage of the MCF-7 cell line, which is deficient for caspase-3 expression (30), enabling the characterization of caspase-8-mediated cleavage of the Bid FRET probe without interference from caspase-3-dependent proteolysis. MCF-7 cells were transfected with a YFP-Bid-CFP FRET probe comprised of YFP, CFP, and the FL-Bid protein as a linker (Fig. 1*A*). Cleavage of FL-Bid results in a separation of YFP and CFP, reducing the efficiency of resonance energy transfer (Fig. 1*A*). Acceptor bleaching experiments were carried out to assess the sensitivity of the FRET probe. The acceptor fluorophore YFP was selectively bleached by repeated scanning of the cell area (Fig. 1*B*, *YFP*). A quantitative analysis of acceptor bleaching showed the absolute fluorescence values for CFP and YFP for a single cell when plotted as a function of time (Fig. 1*C*). Upon bleaching there was a marked decrease in the acceptor fluorescence (YFP), which coincided with an increase in the donor fluorescence (CFP) because of an inability of the acceptor to accept energy from the donor after bleaching. Therefore the increase of CFP fluorescence upon YFP bleaching (Fig. 1, *B* and *C*) confirmed that FRET exists between the two fluorescent proteins in the Bid-FRET probe *in vivo*.

To describe the kinetics of Bid cleavage and translocation during death receptor signaling, MCF-7 cells stably transfected with the Bid-FRET probe were treated with 200 ng/ml TNF-α (+1 μg/ml CHX) to induce caspase-8 activation. Untreated cells showed an evenly distributed CFP and YFP fluorescence within the cell, a stable $\Delta\Psi$m, and normal morphology (Fig. 2*A*). Upon induction of apoptosis the Bid-FRET probe was cleaved, the tBid-CFP fragment was translocated to the mitochondria, and there was a depolarization of the $\Delta\Psi$m (Figs. 2*B* and 4*F*). Following Bid cleavage, tBid-CFP fluorescence was largely clustered at mitochondrial compartments (Fig. 2*C*), and YFP fluorescence was always homogenously distributed throughout the cell.

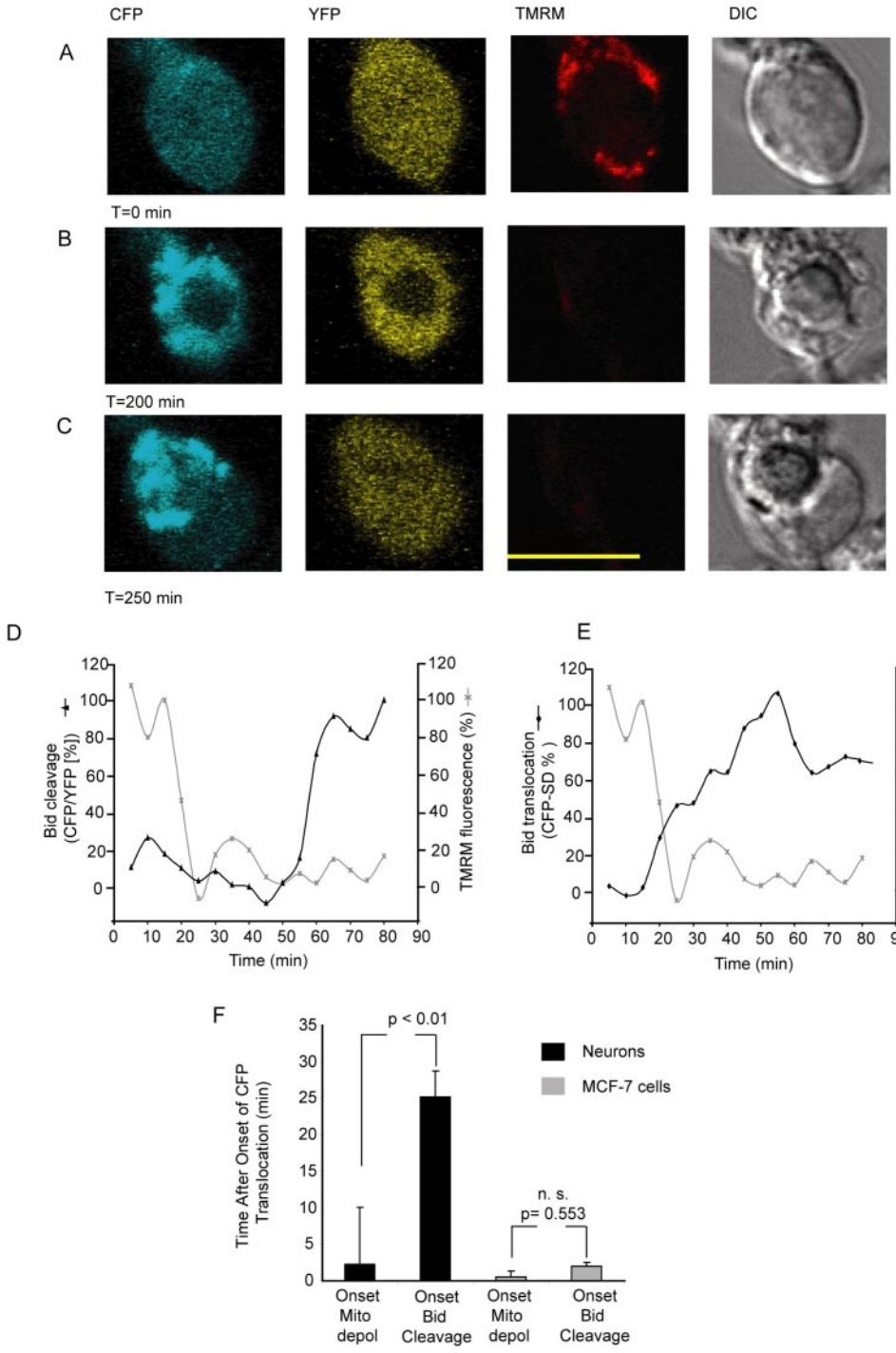

FIGURE 4. **Translocation of FL-Bid and mitochondrial depolarization precede Bid cleavage following transient glutamate receptor overactivation.** Cerebellar granule neurons transiently transfected with a vector encoding the CFP-Bid-YFP FRET probe and loaded with 30 nM TMRM were treated with glutamate/glycine (100 μM/10 μM) for 5 min. After addition of MK-801 (10 μM) to block *N*-methyl-D-aspartate receptor activity the cell was monitored over time with images taken at 5-min intervals and the selected time points (0, 200, and 250 min) shown. *A*, time 0, evenly distributed CFP, YFP fluorescence within the cell, polarized mitochondria (*TMRM*), and normal cellular morphology (*DIC*). *B*, time = 200 min, redistribution of both CFP and YFP fluorescence, depolarization of the $\Delta\Psi$m. *C*, time = 250 min, mitochondrial clustering of CFP fluorescence, re-redistribution of YFP fluorescence to the cytosol, complete depolarization of the $\Delta\Psi$m (*TMRM*) and condensation of the nucleus (*DIC*). *D*, quantitative analysis of Bid translocation (CFP S.D.) and changes in the $\Delta\Psi$m (TMRM fluorescence) following glutamate excitation. *E*, quantitative analysis of Bid cleavage (FRET disruption, CFP/YFP) and changes in the $\Delta\Psi$m (TMRM fluorescence) following glutamate excitation. $n = 7$ cells from seven separate experiments. All neurons that show apoptotic morphology (condensation of the nuclei) following 5-min glutamate receptor overactivation showed an increase in Bid translocation and FRET disruption. (*Bar* = 5 μM). *F*, bar graph showing the onset of $\Delta\Psi$m and Bid cleavage in relation to the onset of Bid translocation for neurons stimulated with glutamate ($n = 7$) and MCF-7 cells ($n = 37$) stimulated with TNF-α/CHX (200 ng/ml/1 μg/ml). $p < 0.01$ difference between onset of mitochondrial depolarization and Bid cleavage in cerebellar granule neurons, no significant difference (*n. s.* $p = 0.553$) was found in MCF-7 cells.

Upon cleavage of the Bid-FRET probe, the CFP/YFP emission ratio increased as a result of FRET disruption. Cleavage kinetics for the Bid-FRET probe were quantified by plotting the CFP/YFP emission ratio as a function of time. The onset of Bid cleavage closely correlated (≤2 min) with the onset of tBid translocation and mitochondrial depolarization (Figs. 2*D* and 4*F*). On average, Bid cleavage occurred 74.5 ± 12.6 min

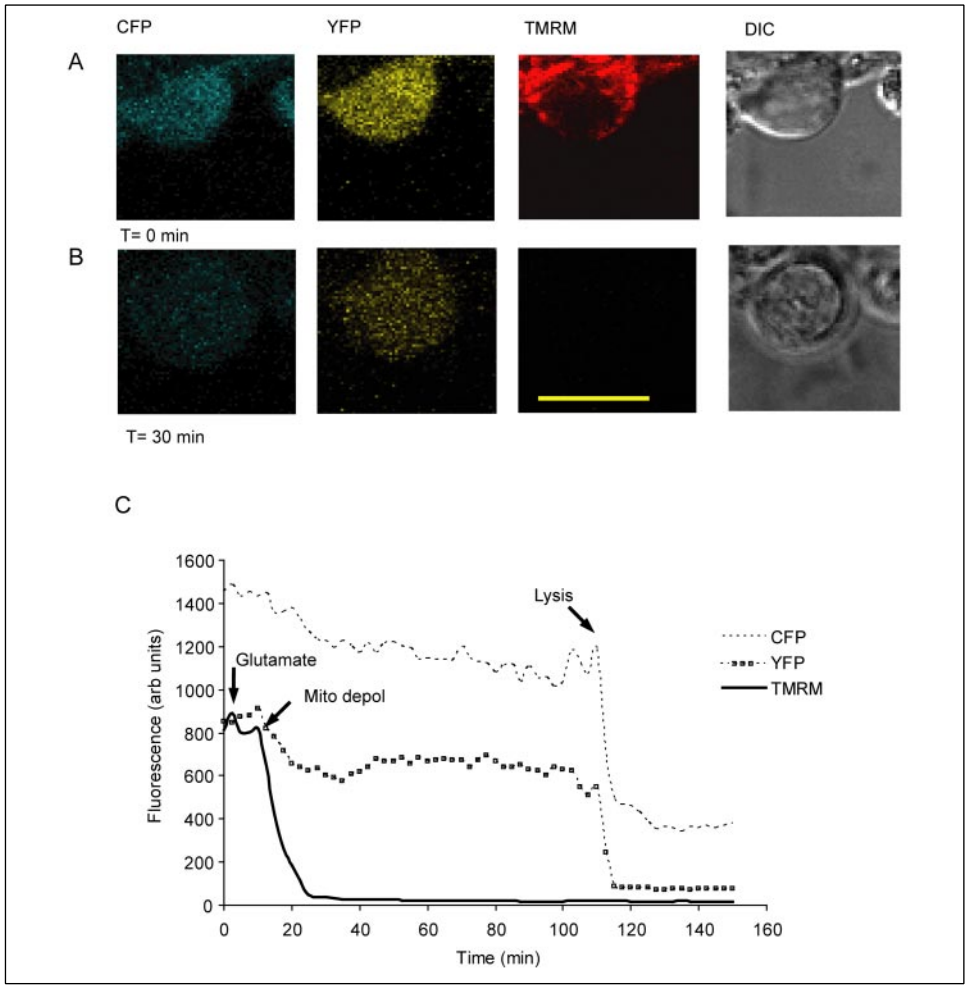

FIGURE 5. **No translocation of Bid or cleavage occurs in cerebellar granule neurons during prolonged glutamate receptor overactivation.** Cerebellar granule neurons transiently transfected with a vector encoding the CFP-Bid-YFP FRET probe and loaded with 30 nM TMRM were exposed continuously to glutamate/glycine (100 μM/10 μM) and monitored over time with images taken at 5-min intervals and the selected time points (0 and 30 min) shown. *A*, time 0, normal cellular morphology (*DIC*), polarized mitochondria (*TMRM*), and evenly distributed CFP and YFP fluorescence within the cell. *B*, time 30 min, enlargement of the nucleus (*DIC*) and swelling of the cell, complete depolarization of the $\Delta\Psi$m. *C*, quantitative analysis of TMRM, CFP and YFP fluorescence during prolonged glutamate excitation. *Arrows* indicate the addition of glutamate, mitochondrial depolarization, and eventual lysis of the neuron. The neuron and traces shown are representative of 5 neurons from five separate experiments.

after stimulus addition (37 cells from $n = 3$ separate experiments). These data show that upon activating apoptotic death receptor signaling the onset of Bid cleavage, tBid translocation and mitochondrial depolarization occur in rapid succession within a narrow time frame.

Transient Glutamate Receptor Overactivation Induces a Delayed Caspase-independent Neuronal Injury—Cerebellar granule neurons have been used extensively to identify acute and long term responses of neurons following glutamate receptor overactivation (31–33). A transient overactivation of the glutamate receptor has been shown to be sufficient to result in a delayed neuronal injury that occurs 2–3 h following the initial insult, which is characterized by a collapse of the $\Delta\Psi$m (32). In this model we induced an overactivation of the glutamate receptors for 5 min (Fig. 3*A*) resulting in a delayed neuronal injury that occurred 4–24 h after the initial exposure (Fig. 3, *B* and *C*). This delayed injury was associated with a collapse in the $\Delta\Psi$m that was closely paralleled with a collapse in Ca^{2+} homeostasis (Fig. 3*B*) and a rapid condensation of the nucleus (Fig. 4, *A* and *B*, *DIC*). In agreement with previously reported studies (21, 22, 24) the apoptotic neuronal injury in this model was not associated with significant activation of effector caspases assayed measuring DEVDase activity. Staurosporine-treated neurons served as a positive control and highlighted the extent to which caspase activation can be induced within cerebellar granule neurons (Fig. 3*D*), indicating that caspase-independent processes are initiated during glutamate-induced apoptosis.

FL-Bid Translocates to the Mitochondria during Excitotoxic Apoptosis in Cerebellar Granule Neurons—Because excitotoxic injury has been shown to require the BH3-only protein Bid (18, 19) we set out to examine in real time, at a single neuron level the role of Bid in our model of caspase-independent, excitotoxic apoptosis. To identify the kinetics of Bid cleavage, cerebellar granule neurons were transiently transfected with the Bid-FRET probe, stimulated with glutamate for 5 min (Fig. 3*A*), and monitored for 24 h. Prior to stimulation the neurons showed an evenly distributed CFP and YFP fluorescence within the cell, a stable $\Delta\Psi$m, and normal morphology (Fig. 4*A*). After glutamate-induced apoptosis (5.6 ± 1.6 h, seven separate experiments) there was a redistribution of both the CFP and YFP fluorescence in the perinuclear region indicating a translocation of FL-Bid-FRET probe to the mitochondria (Fig. 4*B*). This redistribution was paralleled with a depolarization of the $\Delta\Psi$m and a condensation of the nucleus within the cell. After ~20 min the YFP signal became homogenously distributed within the cell, whereas the CFP signal remained clustered in the perinuclear region (Fig. 4*C*), indicating a late cleavage of the Bid-FRET probe.

Following the quantification of the fluorescent signals from neurons stimulated with glutamate for 5 min we were able to identify that the FRET disruption was significantly delayed ($p < 0.01$) in relation to the onset of mitochondrial depolarization (22.9 ± 7.8 min) or translocation of the probe to the mitochondria (25.2 ± 3.5 min) (Fig. 4, *D–F*, seven separate experiments). This was in stark contrast to the results obtained in MCF-7 cells (Figs. 2*D* and 4*F*). It is clear from these responses that a translocation of FL-Bid and a collapse of the $\Delta\Psi$m occur prior to a cleavage of the Bid protein, indicating that Bid cleavage is a secondary event to translocation and mitochondrial depolarization.

We next investigated whether FL-Bid translocation was specific for excitotoxic apoptosis. In previous studies we have used models of con-

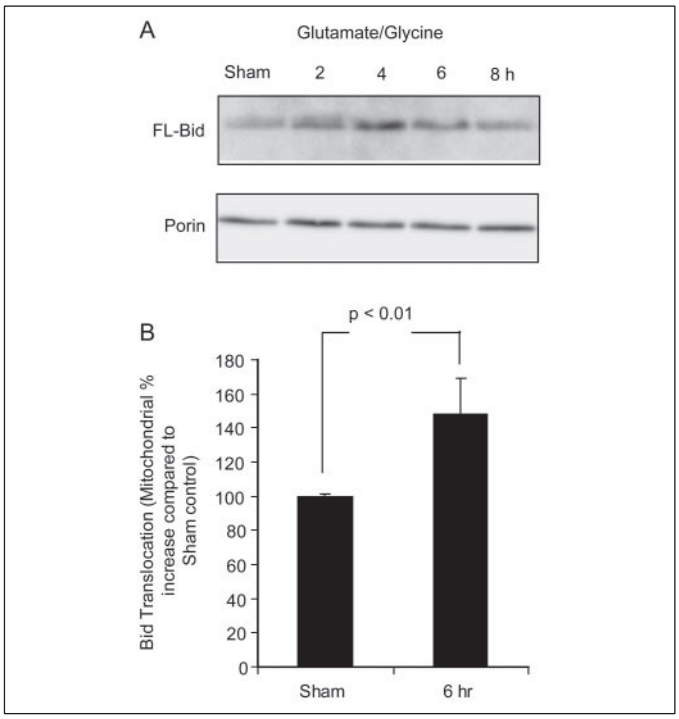

FIGURE 6. **Translocation of FL-Bid from the cytosolic to the mitochondrial fraction during glutamate-induced apoptosis.** *A*, Western blot analysis of FL-Bid distribution in the mitochondrial fraction from neurons that have been treated with glutamate glycine (100 μM/10 μM) for 5 min and harvested 2, 4, 6, and 8 h. Control neurons were treated with buffer only (*sham*). Porin served as a loading control. *B*, quantification of the Western blots. FL-Bid translocation was normalized to porin loading control, and the data were plotted as a percentage of sham-treated neurons ($n = 4$ Western blots, $p < 0.01$).

tinuous glutamate receptor overactivation to induce rapid excitotoxic necrosis within cerebellar granule neurons (31, 32, 34). Cerebellar granule neurons transiently transfected with the Bid-FRET probe were exposed to glutamate continuously (32), and images were taken every 5 min. Prior to stimulation the neurons showed an evenly distributed CFP and YFP fluorescence within the cell, a stable $\Delta\Psi$m, and normal morphology (Fig. 5*A*). After only 30 min of prolonged glutamate exposure there was a collapse of the $\Delta\Psi$m with a rapid swelling of the nucleus and cell body (Fig. 5*B*). No redistribution of CFP or YFP fluorescence occurred under these conditions. Quantification of the fluorescent signals confirmed the absence of any Bid cleavage and translocation during the experiment. Similar results were observed in five separate experiments.

Western Blot Analysis Confirms Translocation of FL-Bid from the Cytosolic to the Mitochondrial Fraction during Glutamate-induced Apoptosis—We employed Western blot analysis to verify whether the transient accumulation of FL-Bid at mitochondria can also be identified within a population of neurons. Cerebellar granule neurons were stimulated with glutamate for 5 min as before (Fig. 3*A*), and the neurons were harvested at several time points following the initial exposure (Fig. 6*A*). A 5-min glutamate stimulus was sufficient to induce a transient increase of FL-Bid in the mitochondrial containing pellet 4–6 h following the initial insult (Fig. 6*A*), a time point where neuronal injury, as measured by LDH release, is starting to increase (Fig. 3*C*). In cerebellar granule neurons transiently transfected with the Bid-FRET probe, cleavage occurred on average 5.9 ± 1.7 h after the initial glutamate exposure. Densitometric analysis of FL-Bid translocation from $n = 4$ separate experiments demonstrated a significant increase in FL-Bid with the mitochondrial pellet at this time point (6 h, Fig. 6*B*).

DISCUSSION

The present study identifies two separate apoptotic pathways where Bid translocation to the mitochondria plays a significant role, caspase-dependent death receptor mediated apoptosis and caspase-independent glutamate-induced apoptosis (12, 13, 21, 22). Death receptor-mediated apoptosis in MCF-7 cells involves the cleavage of FL-Bid, a translocation of tBid to the mitochondria, and a collapse of the $\Delta\Psi$m. In contrast, glutamate-induced apoptosis in cerebellar granule neurons involved a translocation of the FL-Bid to the mitochondria, a depolarization of the $\Delta\Psi$m with a downstream cleavage of the FL-Bid. This study highlights the power of single cell analysis in its ability to identify and resolve the cascade of events that take place within the cell once initiated.

Here we identify that the onset of Bid cleavage, tBid translocation, and mitochondrial depolarization during death receptor-induced apoptosis occur in less than a 2-min time frame in MCF-7 cells. This temporal resolution would have been very difficult to resolve using classical population-based methods. Interestingly, the rapidity of these events parallels to that of cytochrome-*c* and Smac/DIABLO release during apoptosis that we and others have reported previously (35–39) and may help explain the biological nature of these rapid release events. Our results also suggest that very little Bid translocation/cleavage may be sufficient to trigger mitochondrial outer membrane permeabilization during death receptor-induced apoptosis.

Our data also suggest that Bid is involved in additional, caspase-independent pathways such as those triggered intracellularly by the overactivation of glutamate receptors. Here we could demonstrate that glutamate-induced apoptosis involved the translocation of FL-Bid to the mitochondria. No cleavage by caspases (12, 13, 40) or alternative proteases (41, 42) was required for this process. However, alternative proteases such as calpains and cathepsins may be involved in the cleavage of FL-Bid after its translocation to the mitochondria. In this study we identified that the collapse of the $\Delta\Psi$m within our model of glutamate-induced apoptosis was associated with a rapid increase in the cytosolic Ca^{2+} concentration. As calpain activity is highly dependent on the concentration of Ca^{2+} within the cell (43, 44), there is the potential for the activation of calpains following the collapse of the $\Delta\Psi$m within these neurons. Indeed delayed calpain activation has recently been demonstrated in models of excitotoxic neuronal injury (45).

Interestingly, previous reports have demonstrated that the translocation of FL-Bid to the mitochondria may be activated during death receptor-induced apoptosis of Jurkat cells when caspase-8 activation is blocked or during anoikis in epithelial cells (46, 47). Overexpression of FL-Bid or a Bid mutant that cannot be cleaved by caspase-8 was likewise sufficient to activate cell death in Bid- or caspase-8-deficient mouse embryonic fibroblasts (48). It is well established that FL-Bid is capable but less potent than tBid in inducing the release of cytochrome-*c* from isolated mitochondria or permeabilized cells. However, evidence has been presented that changes in the cellular phospholipid content such as increased phosphatidic acid and phosphatidylglycerol levels enhances the ability of FL-Bid to translocate and to permeabilize mitochondria (49). FL-Bid has been shown to insert specific lysophosphatidylcholine species into the membrane surface, thereby triggering the release of apoptogenic factors (50). Interestingly, these alterations in phospholipids have been shown to be a hallmark of excitotoxic, Ca^{2+}-dependent cell death (51). It has also been demonstrated that FL-Bid is able to oligomerize and trigger the insertion of Bax in isolated mitochondria (17). Excitotoxic injury and subsequent changes in phospholipid composition may therefore convert FL-Bid into a "tBid"-like pro-

tein that is subsequently able to activate mitochondrial cell death pathways.

This study demonstrates the power of single cell imaging for the study of protein translocation and protein cleavage during apoptosis. It specifically enhances our understanding of the distinct role of Bid during death receptor mediated caspase-dependent and excitotoxic mediated caspase-independent apoptosis that could be potentially missed in population-based studies.

Acknowledgments—We thank Helena Bonner for technical assistance and Dr. R. Onuki for providing the Bid FRET plasmid.

REFERENCES

1. Bouillet, P., and Strasser, A. (2002) *J. Cell Sci.* **115,** 1567–1574
2. Villunger, A. (2004) *Cell Death Differ.* **11,** 790–793
3. Green, D. R., and Kroemer, G. (2004) *Science* **305,** 626–629
4. Liu, X., Kim, C. N., Yang, J., Jemmerson, R., and Wang, X. (1996) *Cell* **86,** 147–157
5. Zou, H., Henzel, W. J., Liu, X., Lutschg, A., and Wang, X. (1997) *Cell* **90,** 405–413
6. Li, P., Nijhawan, D., Budihardjo, I., Srinivasula, S. M., Ahmad, M., Alnemri, E. S., and Wang, X. (1997) *Cell* **91,** 479–489
7. Wei, M. C., Zong, W. X., Cheng, E. H., Lindsten, T., Panoutsakopoulou, V., Ross, A. J., Roth, K. A., MacGregor, G. R., Thompson, C. B., and Korsmeyer, S. J. (2001) *Science* **292,** 727–730
8. Kuwana, T., Mackey, M. R., Perkins, G., Ellisman, M. H., Latterich, M., Schneiter, R., Green, D. R., and Newmeyer, D. D. (2002) *Cell* **111,** 331–342
9. Goping, I. S., Gross, A., Lavoie, J. N., Nguyen, M., Jemmerson, R., Roth, K., Korsmeyer, S. J., and Shore, G. C. (1998) *J. Cell Biol.* **143,** 207–215
10. Eskes, R., Antonsson, B., Osen-Sand, A., Montessuit, S., Richter, C., Sadoul, R., Mazzei, G., Nichols, A., and Martinou, J. C. (1998) *J. Cell Biol.* **143,** 217–224
11. Huang, D. C., and Strasser, A. (2000) *Cell* **103,** 839–842
12. Gross, A., Yin, X. M., Wang, K., Wei, M. C., Jockel, J., Milliman, C., Erdjument-Bromage, H., Tempst, P., and Korsmeyer, S. J. (1999) *J. Biol. Chem.* **274,** 1156–1163
13. Li, H., Zhu, H., Xu, C. J., and Yuan, J. (1998) *Cell* **94,** 491–501
14. Luo, X., Budihardjo, I., Zou, H., Slaughter, C., and Wang, X. (1998) *Cell* **94,** 481–490
15. Zha, J., Weiler, S., Oh, K. J., Wei, M. C., and Korsmeyer, S. J. (2000) *Science* **290,** 1761–1765
16. Wei, M. C., Lindsten, T., Mootha, V. K., Weiler, S., Gross, A., Ashiya, M., Thompson, C. B., and Korsmeyer, S. J. (2000) *Genes Dev.* **14,** 2060–2071
17. Eskes, R., Desagher, S., Antonsson, B., and Martinou, J. C. (2000) *Mol. Cell Biol.* **20,** 929–935
18. Plesnila, N., Zinkel, S., Le, D. A., Amin-Hanjani, S., Wu, Y., Qiu, J., Chiarugi, A., Thomas, S. S., Kohane, D. S., Korsmeyer, S. J., and Moskowitz, M. A. (2001) *Proc. Natl. Acad. Sci. U. S. A.* **98,** 15318–15323
19. Yin, X. M., Luo, Y., Cao, G., Bai, L., Pei, W., Kuharsky, D. K., and Chen, J. (2002) *J. Biol. Chem.* **277,** 42074–42081
20. Armstrong, R. C., Aja, T. J., Hoang, K. D., Gaur, S., Bai, X., Alnemri, E. S., Litwack, G., Karanewsky, D. S., Fritz, L. C., and Tomaselli, K. J. (1997) *J. Neurosci.* **17,** 553–562
21. Budd, S. L., Tenneti, L., Lishnak, T., and Lipton, S. A. (2000) *Proc. Natl. Acad. Sci. U. S. A.* **97,** 6161–6166
22. Lankiewicz, S., Marc Luetjens, C., Truc Bui, N., Krohn, A. J., Poppe, M., Cole, G. M., Saido, T. C., and Prehn, J. H. (2000) *J. Biol. Chem.* **275,** 17064–17071
23. Johnson, M. D., Kinoshita, Y., Xiang, H., Ghatan, S., and Morrison, R. S. (1999) *J. Neurosci.* **19,** 2996–3006
24. Cao, J., Semenova, M. M., Solovyan, V. T., Han, J., Coffey, E. T., and Courtney, M. J. (2004) *J. Biol. Chem.* **279,** 35903–35913
25. Takano, J., Tomioka, M., Tsubuki, S., Higuchi, M., Iwata, N., Itohara, S., Maki, M., and Saido, T. C. (2005) *J. Biol. Chem.* **280,** 16175–16184
26. Ward, M. W., Kushnareva, Y., Greenwood, S., and Connolly, C. N. (2005) *J. Neurochem.* **92,** 1081–1090
27. Onuki, R., Nagasaki, A., Kawasaki, H., Baba, T., Uyeda, T. Q., and Taira, K. (2002) *Proc. Natl. Acad. Sci. U. S. A.* **99,** 14716–14721
28. Rehm, M., Dussmann, H., Janicke, R. U., Tavare, J. M., Kogel, D., and Prehn, J. H. (2002) *J. Biol. Chem.* **277,** 24506–24514
29. Slee, E. A., Keogh, S. A., and Martin, S. J. (2000) *Cell Death Differ.* **7,** 556–565
30. Janicke, R. U., Sprengart, M. L., Wati, M. R., and Porter, A. G. (1998) *J. Biol. Chem.* **273,** 9357–9360
31. Budd, S. L., and Nicholls, D. G. (1996) *J. Neurochem.* **67,** 2282–2291
32. Ward, M. W., Rego, A. C., Frenguelli, B. G., and Nicholls, D. G. (2000) *J. Neurosci.* **20,** 7208–7219
33. Castilho, R. F., Hansson, O., Ward, M. W., Budd, S. L., and Nicholls, D. G. (1998) *J. Neurosci.* **18,** 10277–10286
34. Castilho, R. F., Ward, M. W., and Nicholls, D. G. (1999) *J. Neurochem.* **72,** 1394–1401
35. Waterhouse, N. J., Goldstein, J. C., von Ahsen, O., Schuler, M., Newmeyer, D. D., and Green, D. R. (2001) *J. Cell Biol.* **153,** 319–328
36. Dussmann, H., Rehm, M., Kogel, D., and Prehn, J. H. (2003) *J. Cell Sci.* **116,** 525–536
37. Heiskanen, K. M., Bhat, M. B., Wang, H. W., Ma, J., and Nieminen, A. L. (1999) *J. Biol. Chem.* **274,** 5654–5658
38. Goldstein, J. C., Waterhouse, N. J., Juin, P., Evan, G. I., and Green, D. R. (2000) *Nat. Cell Biol.* **2,** 156–162
39. Rehm, M., Dussmann, H., and Prehn, J. H. (2003) *J. Cell Biol.* **162,** 1031–1043
40. Wagner, K. W., Engels, I. H., and Deveraux, Q. L. (2004) *J. Biol. Chem.* **279,** 35047–35052
41. Chen, M., He, H., Zhan, S., Krajewski, S., Reed, J. C., and Gottlieb, R. A. (2001) *J. Biol. Chem.* **276,** 30724–30728
42. Mandic, A., Viktorsson, K., Strandberg, L., Heiden, T., Hansson, J., Linder, S., and Shoshan, M. C. (2002) *Mol. Cell Biol.* **22,** 3003–3013
43. Saido, T. C., Sorimachi, H., and Suzuki, K. (1994) *FASEB J.* **8,** 814–822
44. Inomata, M., Hayashi, M., Nakamura, M., Imahori, K., and Kawashima, S. (1985) *J. Biochem.* (*Tokyo*) **98,** 407–416
45. Bano, D., Young, K. W., Guerin, C. J., Lefeuvre, R., Rothwell, N. J., Naldini, L., Rizzuto, R., Carafoli, E., and Nicotera, P. (2005) *Cell* **120,** 275–285
46. Tafani, M., Karpinich, N. O., Hurster, K. A., Pastorino, J. G., Schneider, T., Russo, M. A., and Farber, J. L. (2002) *J. Biol. Chem.* **277,** 10073–10082
47. Valentijn, A. J., and Gilmore, A. P. (2004) *J. Biol. Chem.* **279,** 32848–32857
48. Sarig, R., Zaltsman, Y., Marcellus, R. C., Flavell, R., Mak, T. W., and Gross, A. (2003) *J. Biol. Chem.* **278,** 10707–10715
49. Esposti, M. D., Erler, J. T., Hickman, J. A., and Dive, C. (2001) *Mol. Cell Biol.* **21,** 7268–7276
50. Goonesinghe, A., Mundy, E. S., Smith, M., Khosravi-Far, R., Martinou, J. C., and Esposti, M. D. (2005) *Biochem. J.* **387,** 109–118
51. Gasull, T., DeGregorio-Rocasolano, N., Zapata, A., and Trullas, R. (2000) *J. Biol. Chem.* **275,** 18350–18357

Real Time Single Cell Analysis of Bid Cleavage and Bid Translocation during Caspase-dependent and Neuronal Caspase-independent Apoptosis

Manus W. Ward, Markus Rehm, Heiko Duessmann, Slavomir Kacmar, Caoimhin G. Concannon and Jochen H. M. Prehn

J. Biol. Chem. 2006, 281:5837-5844.
doi: 10.1074/jbc.M511562200 originally published online December 28, 2005
